Biogeosciences Discuss., 11, 5903–5939, 2014
www.biogeosciences-discuss.net/11/5903/2014/
doi:10.5194/bgd-11-5903-2014

Biogeosciences
Discussions
Open Access

Constraint of soil moisture on CO_2 efflux from tundra lichen, moss, and tussock in Council, Alaska using a hierarchical Bayesian model

Y. Kim[1], K. Nishina[2], N. Chae[3], S. Park[4], Y. Yoon[5], and B. Lee[5]

[1]International Arctic Research Center, University of Alaska Fairbanks, AK 99775-7335, USA
[2]Center for Regional Environmental Research, National Institute for Environmental Studies, Tsukuba, 305-8506, Japan
[3]Civil and Environmental Engineering, Yonsei University, Seoul 120-749, Korea
[4]Division of Climate Change, Korea Polar Research Institute (KOPRI), Incheon 406-840, Korea
[5]Arctic Research Center, Korea Polar Research Institute (KOPRI), Incheon 406-840, Korea

Received: 3 March 2014 – Accepted: 7 April 2014 – Published: 25 April 2014

Correspondence to: Y. Kim (kimyw@iarc.uaf.edu)

Published by Copernicus Publications on behalf of the European Geosciences Union.

Abstract

The tundra ecosystem is quite vulnerable to drastic climate change in the Arctic, and the quantification of carbon dynamics is of significant importance in response to thawing permafrost, changes in the snow-covered period and snow and shrub community extent, and the decline of sea ice in the Arctic. Here, CO_2 efflux measurements using a manual chamber system within a 40 m × 40 m (5 m interval; 81 total points) plot were conducted in dominant tundra vegetation on the Seward Peninsula of Alaska, during the growing seasons of 2011 and 2012, for the assessment of the driving parameters of CO_2 efflux. We applied a hierarchical Bayesian (HB) model – which is a function of soil temperature, soil moisture, vegetation type and thaw depth – to quantify the effect of environmental parameters on CO_2 efflux, and to estimate growing season CO_2 emission. Our results showed that average CO_2 efflux in 2011 is 1.4-fold higher than in 2012, resulting from the distinct difference in soil moisture between the two years. Tussock-dominated CO_2 efflux is 1.4 to 2.3 times higher than those measured in lichen and moss communities, reflecting tussock as a significant CO_2 source in the Arctic, with wide area distribution on a circumpolar scale. CO_2 efflux followed soil temperature nearly exponentially from both the observed data and the posterior medians of the HB model. This reveals soil temperature as the most important parameter in regulating CO_2 efflux, rather than soil moisture and thaw depth. Obvious changes in soil moisture during the growing seasons of 2011 and 2012 resulted in an explicit difference in CO_2 efflux – 742 and 539 g CO_2 m^{-2} $period^{-1}$ in 2011 and 2012, respectively, suggesting that the 2012 CO_2 emission rate was constrained by 27 % (95 % credible interval: 17–36 %) compared to 2011, due to higher soil moisture from severe rain. Estimated growing season CO_2 emission rate ranged from 0.86 Mg CO_2 $period^{-1}$ in 2012 to 1.2 Mg CO_2 $period^{-1}$ in 2011 within a 40 m × 40 m plot, corresponding to 86 % and 80 % of the annual CO_2 emission rates within the Alaska western tundra ecosystem. Therefore, the HB model can be readily applied to observed CO_2 efflux, as it demands

BGD
11, 5903–5939, 2014

only four environmental parameters and can also be effective for quantitatively assessing the driving parameters of CO_2 efflux.

1 Introduction

Carbon dioxide (CO_2) efflux from the soil surface to the atmosphere is important for estimating regional and global carbon budgets (Schlesinger and Andrews, 2000; Bond-Lamberty and Thomson, 2010), and is susceptible to increasing air temperature (Bond-Lamberty and Thomson, 2010), to the degradation of permafrost (Schuur et al., 2009; Jensen et al., 2014), and to the expansion of the shrub community (Sturm et al., 2005). This suggests stimulation of the terrestrial carbon cycle response to drastic climate change in the Arctic (ACIA, 2004).

The tundra ecosystem of Alaska has received attention for the enhanced greening in abundant Arctic coastal shrubs that has come with the decline of sea ice (Bhatt et al., 2010, 2013; Post et al., 2013), the shortened snow-covered period (Hinzman et al., 2005), thawing permafrost and shrinking ponds and lakes (Romanovsky et al., 2002; Yoshikawa and Hinzman, 2003; Hinzman et al., 2005; Smith et al., 2005), all reflecting the changes in terrestrial carbon and water cycles (Davidson et al., 1998; Oechel et al., 2000; Michaelson and Ping, 2003; ACIA, 2004; Oberbauer et al., 2007; Walter et al., 2007; Koven et al., 2011). Recently, Jensen et al. (2014) found a distinct difference in CO_2 efflux from undisturbed tundra during 2011 and 2012, resulting from greater rainfall in the growing season of 2012. This suggests that higher soil moisture from rainfall is a suppressant parameter for releasing soil-produced CO_2 emitted to the atmosphere (Davidson et al., 1998; Oberbauer et al., 2007), decreasing CO_2 emission by 43 % (Jensen et al., 2014). Davidson et al. (1998) reported CO_2 efflux increased with soil moisture of 0.2 $m^3\,m^{-3}$, then steadily decreasing with increasing soil moisture content beyond 0.2 $m^3\,m^{-3}$. Hence, the magnitude of CO_2 efflux depends profoundly on the extent of soil moisture. Further, soil temperature is well known as a significant parameter for regulating CO_2 efflux in worldwide terrestrial ecosystems, as reported by many researchers (Davidson et al., 1998; Xu and Qi, 2001; Davidson and Janssens, 2006; Rayment and Jarvis, 2000; Kim et al., 2007, 2013; Jensen et al., 2014). Q_{10} value, which is a measure of the change in reaction rate at intervals of 10 °C (Lloyd and Taylor, 1994), has been effectively used to understand the temperature sensitivity of soil microbial activity as an exponential function (Davidson et al., 1998; Xu and Qi, 2001; Monson et al., 2006; Bond-Lamberty and Thomson, 2010; Kim et al., 2013). For example, Monson et al. (2006) estimated the highest Q_{10} value of 1.25×10^6 as the beneath-snowpack soil temperature warmed from −3 to 0 °C in a high-elevation subalpine forest in Colorado, reflecting the higher CO_2 production by beneath-snow microbes, such as snow molds, in the end winter and early spring season. Therefore, soil temperature, which is an analogue of soil microbial activity, is the most important parameter in producing CO_2 in the soil.

Monthly CO_2 efflux measured in the tundra ecosystem has been further recognized as having insufficient spatiotemporal resolution and representativeness of efflux data with the conventional dynamic chamber method (Hutchinson and Livingston, 2002; Savage and Davidson, 2003). If spatial distribution is not normal distribution, the ensemble average flux will likely cause estimation bias (Clark, 2005). In order to overcome the weakness of monthly CO_2 efflux measurement in the field, the hierarchical Bayesian (HB) model framework can be applied for estimation of CO_2 efflux from the tundra ecosystem, as Clark (2005) and Nishina et al. (2009, 2012) used. Their results indicated the HB model is an effective tool for the estimation of fluxes and evaluation of environmental parameters with less bias. Lately, free software such as WinBUGS (http://www.mrc-bsu.ac.uk/bugs) has resulted in the availability of a HB model using the Markov Chain Monte Carlo (MCMC) method (Spiegelhalter and Best, 2000). Clark (2005) described that the HB model reveals complex nonlinear relationships between efflux and environmental parameters.

In this study, we modeled observed CO_2 efflux using a HB model with four explanatory variables: soil temperature, soil moisture, vegetation types, and thaw depth, under the assumption of the lognormal distribution. The HB model used in this study

BGD
11, 5903–5939, 2014

accommodated nonlinear relationships between the efflux and environmental parameters. Therefore, the objectives of this study are (1) to evaluate the characteristics of dominant plants on CO_2 efflux; (2) to quantitatively assess driving factors of CO_2 efflux simulated by a hierarchical Bayesian (HB) model; and (3) to estimate the growing season CO_2 emission rate within a 40 m × 40 m plot in the western Alaska tundra ecosystem.

2 Materials and methods

2.1 Study site and experimental methods

The study site is dominantly covered by typical tussock tundra. This site is located at the community of Council (64°51′38.3″ N; 163°42′39.7″ W; 45 m a.s.l.), on the Seward Peninsula, about 120 km northeast of Nome, Alaska. This site was selected for its relatively smooth transition from forest to tundra, with underlying discontinuous permafrost regime. The monthly average air temperature of 1.2 °C at the Nome airport from 1971 to 2010 ranged from −10.5 °C in January to 14.6 °C in July. Annual average precipitation was 427 mm, including snowfall (Western Regional Climate Center). During the growing seasons (June to September) of 2011 and 2012, average ambient temperature and precipitation were 8.9 ± 1.0 °C (CV, coefficient of variance: 12 %) and 285 mm, and 8.5 ± 2.8 °C (CV: 33 %) and 380 mm, respectively, as shown in Fig. 1. Precipitation in July-August of 2011 and 2012 were 231 and 299 mm, corresponding to 81 and 79 % of growing season precipitation. Under heavy precipitation in early July of 2011, CO_2 efflux-measurement could unfortunately not be conducted, due to underestimation of CO_2 efflux. The sampling period was 17–24 June, 2–8 August, and 9–15 September for 2011, and 20–29 June, 14–21 July, 11–18 August, and 8–15 September for 2012. The DOT (Department of Transportation) of Alaska has maintained the access road from Nome to Council, open from late May to late September. Because this access road was closed during the snow-covered period (October to May), CO_2 efflux-

BGD
11, 5903–5939, 2014

Title Page
Abstract | Introduction
Conclusions | References
Tables | Figures
◄ | ►
◄ | ►
Back | Close
Full Screen / Esc
Printer-friendly Version
Interactive Discussion

measurement could not be conducted during non-growing season. The Council site has been managed by the WERC (Water Environmental Research Center) of UAF (University of Alaska Fairbanks) since 1999, for changes in permafrost and the water cycle (Yoshikawa and Hinzman, 2003).

This study determined CO_2 efflux and environmental factors in lichen-, moss- and tussock- dominant tundra microsites within a 40 m × 40 m plot (5 m interval; 81 points) at this site during the growing seasons of 2011 and 2012. Our plot was established for better understanding of spatiotemporal variations of CO_2 efflux and environmental data. Within the 81-point area, on-ground dominant plants are lichen (*Cladonia mitis*, *Cladonia crispata,* and *Cladonia stellaris*); moss, such as sphagnum (*Sphagnum magellanicum*, *Sphagnum angustifolium,* and *Sphagnum fuscum*) and others (*Polytricum* spp., *Thuidium abietinum*, and *Calliergon* spp.); and cotton grass tussock tundra (*Eriophorum vaginatum*). Dominant lichen, moss, and tussock tundra were occupied the plot at 27, 53, and 20 % within the plot, respectively.

Soil temperatures were taken at 5 and 10 cm below the surface using a portable thermometer with two probes (Model 8402-20, Cole-Palmer, USA), and soil moisture was measured at each point with a portable soil-moisture logger (HH2, Delta-T Devices, UK) with sensor (ML2, Delta-T Devices, UK). Thaw depth was measured with a fiberglass tile probe (1.5 m long), and pH with a waterproof meter (IQ 160, Ben Meadows, USA) in September of 2011 for soil characteristics. A one-way or two-way ANOVA (95 % confidence level) and regression analysis of data using Microsoft Excel Data Analysis software were performed.

2.2 Estimation of CO_2 efflux

Our dynamic CO_2 efflux-measuring system used was portable, convenient, and capable of calculating efflux in situ. The 81-cylindrical chamber base (30 cm dia., 40 cm high) was fixed to the surface within each point. The system consisted of a transparent-material chamber lid (35 cm dia., 0.3 cm thick) with input and output urethane tubing (6 mm OD; 4 mm ID), and a pressure vent; a commercial pump (CM-15-12, Enomoto

BGD
11, 5903–5939, 2014

Micro Pump Co., Ltd., Japan); a NDIR CO_2 analyzer (Licor-820, LICOR Inc., USA); a commercial 12 V battery; and a laptop computer for efflux calculation (Kim et al., 2013). This system is similar to the manual system of Savage and Davidson (2003; see Fig. 1). To minimize the effect of pressure inside the chamber, the flow rate of the pump maintained a rate of 0.5 L min^{-1}, due to underestimation or overestimation of CO_2 efflux by under-pressurization or over-pressurization of the used chamber and caused by flow restrictions in air circulating design (Davidson et al., 2002). The efflux-measuring time at a point was at a 5–10 min interval, depending on weather and soil surface conditions. For CO_2 efflux in the tussock estimates, the surface area is variable and dependent on height; average tussock height in this case is 18.7 ± 5.1 cm (CV: 27 %).

Efflux was calculated from the following equation, as described by Kim et al. (2013):

$$F_{CO_2} = \rho_a \times (\Delta C/\Delta t) \times (V/A), \quad (1)$$

where F_{CO_2} is the measured soil CO_2 efflux (g CO_2 m^{-2} min^{-1}), ρ_a is the molar density of dry air (mol m^{-3}), ΔC (ppmv) is the change in CO_2 concentration during measuring time (Δt, 5 to 10 min), V is chamber volume, and A is surface area (cross section = 0.070 m^2). The height of each chamber was also measured alongside the chamber to allow calculation of the efflux.

To assess the response of temperature dependence on CO_2 efflux, the relationship was plotted and showed exponential curves for soil temperature at depths of 5 and 10 cm from this equation:

$$F_{CO_2} = \beta_0 \times e^{\beta_1 \times T}, \quad (2)$$

where T is soil temperature (°C), and β_0 and β_1 are constants. This exponential relationship is commonly used to represent soil carbon efflux as a function of temperature (Davidson et al., 1998; Xu and Qi, 2001; Davidson and Janssens, 2006; Rayment and Jarvis, 2000; Kim et al., 2007, 2013). The Q_{10} temperature coefficient values were

BGD
11, 5903–5939, 2014

calculated as in Davidson et al. (1998) and Kim et al. (2013):

$$Q_{10} = e^{\beta_1 \times 10}. \tag{3}$$

Q_{10} is a measure of the change in reaction rate at intervals of 10 °C and is based on Van't Hoff's empirical rule that a rate increase on the order of 2 to 3 times occurs for every 10 °C rise in temperature (Lloyd and Taylor, 1994).

2.3 Description of Hierarchical Bayesian (HB) model

In a HB model, to evaluate the relationship between CO_2 efflux and environmental variables, we modeled observed CO_2 efflux using a HB model with four explanatory variables: soil temperature (ST), soil moisture (SM), vegetation types (Vege), and thaw depth (THAW), based on Nishina et al. (2009, 2012).

First, CO_2 efflux (F_{CO_2}) was assumed to be normally distributed with mean parameter (μ_{flux}) and variance parameter (σ):

$$F_{CO_2} \sim \mathrm{normal}(\mu_{flux}, \sigma^2), \tag{4}$$

The scale parameter (μ_{flux}) was determined from the following equation:

$$\mu_{flux} = f_P f_{ST} f_{SM} f_{THAW}, \tag{5}$$

where f_P represents the function of CO_2 efflux potential, and f_{ST} and f_{SM} are limiting response functions that ranged from 0 to 1. f_P was defined as follows:

$$f_P = \beta_0 + \mathrm{Vege}_{[k]} + \mathrm{Year}_{[l]}. \tag{6}$$

f_P is a linear predictor that has three parameters ("β_0", "β_1", "β_2").

Temperature (f_{ST}) is a modified Van't Hoff equation, as follows:

$$f_{ST} = e^{\frac{ST - ST_{ref}}{10}\log(Q_{tem})}, \tag{7}$$

BGD
11, 5903–5939, 2014

where f_{ST} is the temperature response function, which varies from 0 to 1. The explanatory variable of this function, represented by ST and ST_{ref}, is a constant, set at 30 °C in this study. The temperature sensitivity parameter is Q_{tem}. The soil moisture liming function (f_{SM}) is defined as follows:

$$f_{SM} = \left(\frac{\text{WFPS} - a}{b - a}\right)^{a} \left(\frac{\text{WFPS} - c}{b - c}\right)^{-d(b-c)/(b-a)}, \tag{8}$$

where the soil moisture response function is f_{SM}, ranging from 0 to 1, and is the same as the temperature response function. WFPS is the explanatory variable of this function, and a, b, and c are the parameters.

f_{THAW} is a function of thaw depth. We modeled this as follows:

$$f_{THAW} = \frac{1}{1 + e^{k - r\text{THAW}}}, \tag{9}$$

where thaw depth function also ranges from 0 to 1. THAW is the explanatory variable in this function; k and r are the parameters. We assumed that CO_2 efflux monotonically increases with an increase in thaw depth (e.g., depth of active layer); however, this increase is not simply proportional with thaw depth, due to carbon depth distribution.

Finally, we modeled the priors of each parameter. For vegetation, we incorporated a random effect as follows:

$$\text{Vege}_i \sim \text{normal}(0, \sigma_{vege}); \tag{10}$$

$$\text{Year}_i \sim \text{normal}(0, \sigma_{year}). \tag{11}$$

For priors, we defined as follows:

$$\beta_0 \sim \text{normal}(0, 1000),$$
$$Q_{10} \sim \text{uniform}(1, 10),$$
$$a \sim \text{uniform}(-2, 0),$$

BGD
11, 5903–5939, 2014

Constraint of soil moisture on CO_2 efflux in tundra ecosystem

Y. Kim et al.

$$
\begin{aligned}
&b \sim \mathrm{uniform}(0.1, 0.5),\\
&c \sim \mathrm{uniform}(1, 3),\\
&d \sim \mathrm{uniform}(0.01, 10),\\
&k \sim \mathrm{uniform}(0, 10),\\
&r \sim \mathrm{uniform}(0, 1),\\
&\sigma^2 \sim \mathrm{uniform}(0, 100),\\
&\sigma^2_{\mathrm{vege}} \sim \mathrm{uniform}(0, 100), \text{ and}\\
&\sigma^2_{\mathrm{year}} \sim \mathrm{uniform}(0, 100).
\end{aligned}
\tag{12}
$$

For β_0, β_1, and β_2, we used a normal distribution with mean 0 and a very large variance. The joint posterior probability was described as follows:

$$
\begin{aligned}
p(\theta|\mathrm{data}) \propto \prod \mathrm{Normal}(F_{CO_2}|\mu, \beta_{o,10}, a, b, c, d, k, r, \sigma_1, \sigma_{\mathrm{vege}}, \sigma_{\mathrm{year}})\\
\times p(\beta_o) \times p(Q_{10}) \times p(a) \times p(b) \times p(c) \times p(d) \times p(k) \times p(r),
\end{aligned}
\tag{13}
$$

where $p(\theta)$ denotes priors. For this model, we used MCMC (Markov Chain Monte Carlo) methods implemented with Bayesian inference using the Gibbs sampling software JAGS/WinBUGS (Spiegelhalter and Best, 2000: WinBUGS, version 1.4.3, 2007, available at http://www.mrc-bsu.ac.uk/bugs). We used the Gelman–Rubin convergence diagnostic as an index. For the model, we ran the Gibbs sampler for 20 000 iterations for three chains, with a thinning interval of 10-iternation. We discarded the first 10 000 iterations as burn-in and used the remaining iterations to calculate posterior estimates. The R (R Development Core Team, 2012) was used to call JAGS/WinBUGS and calculate statistics in R.

BGD
11, 5903–5939, 2014

3 Results and discussion

3.1 CO_2 efflux and environmental parameters

Table 1 shows monthly average ± standard deviation (coefficient of variance, %) of CO_2 efflux, soil temperature at 5 and 10 cm depth below the surface, soil moisture, thaw depth, and pH in lichen, moss, tussock tundra, and grass during the growing seasons of 2011 and 2012. Growing season-averaged CO_2 effluxes of 2011 and 2012 are 3.6±2.7 (75 %) and 3.2 ± 1.7 (53 %) mg CO_2 m^{-2} min^{-1} in lichen (n = 166), 4.5 ± 2.9 (65 %) and 3.9 ± 1.9 (49 %) mg CO_2 m^{-2} min^{-1} in moss (n = 278), 7.2 ± 5.7 (79 %) and 5.0 ± 2.6 (51 %) mg CO_2 m^{-2} min^{-1} in tussock tundra (n = 103), 4.8 ± 2.2 (46 %) and 4.4 ± 2.2 (50 %) mgCO_2 m^{-2} min^{-1} in grass (n = 30). Annual average CO_2 efflux is 4.6 ± 2.5 (54 %) and 3.1 ± 2.0 (66 %) mg CO_2 m^{-2} min^{-1} for 2011 and 2012, respectively. This indicates the growing season CO_2 efflux in 2011 was 1.5-time higher than 2012, also indicating the significance of heavy rainfall in the mid-growing season of 2012. CO_2 efflux in tussock tundra was approximately 1.8 times greater than in other plants, which may be due more to the relatively wider surface area than others. While surface area in lichen and moss is 0.070 m^2, the same surface area of the measurement chamber, average surface area is 0.090 ± 0.024 m^2, based on average tussock height of 19.2 ± 5.1 cm. CO_2 efflux in the Arctic tundra of Alaska ranged from 0.38 to 1.6 mg CO_2 m^{-2} min^{-1} in lichen and 0.44 to 4.3 mg CO_2 m^{-2} min^{-1} in tussock during the growing season (Poole and Miller, 1982). In tundra near Barrow, Alaska, Oechel et al. (1997) reported 0.76 and 0.20 mg CO_2 m^{-2} min^{-1} in tussock tundra and wet sedge, suggesting that CO_2 efflux in tussock is a significant atmospheric CO_2 source, ten times greater than in wet sedge. The surface area of the chamber used by Oechel et al. (1997) was 0.56 m^2, which is an order of magnitude higher than that used in this study. Kim et al. (2013) reported that tussock is an important source of carbon efflux to the atmosphere, contributing 3.4-fold more than other vegetation types in Alaska tundra and boreal forest systems. Further, tussock-originated CO_2 efflux, which occupies a circumpolar area

BGD
11, 5903–5939, 2014

ranging from 9×10^{11} m^2 (Miller et al., 1983) to 6.5×10^{12} m^2 (Whalen and Reeburgh, 1988) when counted with moss species, provides a quantitative understanding of a significant atmospheric carbon source from the Arctic terrestrial ecosystem. Considering the circumpolar distribution of tussock tundra and moss in the Arctic tundra ecosystem, the CO_2 efflux measured in this study should not be overlooked in the evaluation of the regional/global carbon budget regarding distribution characteristics of on-ground plants. Spatial distribution of CO_2 efflux within a 40 m × 40 m plot in 2011 and 2012, as shown in Fig. 2. CO_2 efflux in June 2011 was much higher than other observation periods, reflecting higher air temperature and lower precipitation in June (see Fig. 1). This suggests the explicit difference in CO_2 efflux in June of 2011 and 2012 within the plot, as shown in Table 1. CO_2 efflux in September 2012 rapidly decreased due to heavy rainfall from mid-August to mid-September 2012. Within the plot, while the CV of monthly average CO_2 efflux in 2011 is prone to decrease, the CV in 2012 tends to increase. This denotes the susceptibility to extreme environmental parameters in 2012, compared to 2011.

Annual growing season average ± standard deviation soil temperatures at 5 and 10 cm below the soil surface were 9.0 ± 4.2 (47 %) and 5.9 ± 3.9 °C (66 %) for 2011, and 7.7 ± 4.5 (58 %) and 5.7 ± 3.5 °C (61 %) for 2012, respectively, as shown in Fig. 3. This denotes soil temperature in 2011 is higher than 2012, as shown in annual average CO_2 efflux, suggesting soil temperature is likely to modulate CO_2 efflux, as reported considerably in regions worldwide (Davidson et al., 1998; Xu and Qi, 2001; Davidson and Janssens, 2006; Rayment and Jarvis, 2000; Kim et al., 2007, 2013). The spatial distribution of high/low soil temperature for each month was identical to the pattern of high/low CO_2 efflux, as shown in Fig. 2.

Annual average soil moisture was 0.253 ± 0.158 (CV: 62 %) m^3 m^{-3} in 2011, and 0.272 ± 0.180 m^3 m^{-3} (66 %) in 2012, indicating moisture in 2011 is slightly lower than in 2012 (not shown). Soil moisture in September 2011 was not measured, due to broken soil moisture sensor. Spatial distribution of soil moisture is related to geographical topography, such as slope and relief within the plot, reflecting spatial distribution of

BGD
11, 5903–5939, 2014

lower CO_2 efflux and lower soil temperature in the trough area (not shown). Soil moisture, along with soil temperature, is also an important factor in controlling CO_2 efflux (Davidson et al., 1998; Gaumont-Guay et al., 2006; Mahecha et al., 2010; Kim et al., 2013).

Average thaw depth was 39 ± 5 (15 %) cm in 2011 and 38 ± 6 (15 %) cm in 2012, showing no significantly difference, based on a one-way ANOVA at the 95 % confidence level. The distribution of thaw depth (not shown) seems similar to the pattern of soil moisture, though not related to those of CO_2 efflux and soil temperature. The average thaw rate over our 81 points is $0.43\,\mathrm{cm\,day^{-1}}$ in 2011 and $0.41\,\mathrm{cm\,day^{-1}}$ in 2012 as shown in Fig. 4, reflecting that thaw rate with time is almost constant during the growing season, and that thaw depth is not thought to regulate CO_2 efflux. In general, the deeper the active layer in response to permafrost thaw in the Arctic (Marchenko et al., 2008), the more CO_2 emission from the soil to the atmosphere (Elberling et al., 2013), also suggesting the potential decomposition of frozen, higher stocked soil organic carbon (Ping et al., 2008; Tarnocai et al., 2009; Grosse et al., 2011). However, temporal variation in thaw depth of the active layer may not stimulate CO_2 production. This suggests that the strength of CO_2 production that depends on the soil microbial metabolism is affected more by environmental parameters than the constant active layer depth for both years. The deeper active layer reached to nearly 80 cm below the surface with the profile of soil temperature at 50, 70, 80, and 92 cm from July 2012 to October 2013 (not shown). When the soil contained much higher soil moisture and much deeper thaw depth for September, pH represented a similar value of 3.8 ± 0.4 (11 %), representing an acidic tundra soil (pH < 5.5; Walker et al., 1998), among all points. The pH measurement was not conducted during the growing season of 2012, due to almost uniformity within the plot.

3.2 Environmental parameters determining CO_2 efflux

CO_2 efflux is possibly modulated by environmental factors such as soil temperature, soil moisture, and thaw depth. Q_{10} values were calculated using Eq. (3), which is based on the exponential relationship between CO_2 efflux and soil temperature at 5 and 10 cm depths for each plant. Table 2 shows Q_{10} values and correlation coefficients between CO_2 efflux and soil temperature at 5 and 10 cm depths in lichen, moss, grass, and tussock tundra during the growing season, based on a one-way ANOVA with a 95 % confidence level. Q_{10} is prone to increasing with time, suggesting that CO_2 production by soil microbes and roots has greater sensitivity to a narrower range of soil temperatures, such as in the spring and fall seasons (Rayment and Jarvis, 2000; Gaumont-Guay et al., 2006; Monson et al., 2006; Malcom et al., 2009). In this Alaska tundra ecosystem, average daily CO_2 efflux from wet sedge followed soil surface temperature closely, increasing exponentially as soil surface temperature increased, while efflux from the tussock tundra ecosystem followed soil surface temperature nearly logarithmically (Oechel et al., 1997). In this study, the response from CO_2 efflux in tussock tundra on soil temperature depicts an almost linear relationship; however, it shows an exponential curve for Q_{10} values, listed in Table 2. Soil temperature at 5 cm depth explained 86 and 70 % of the variability in CO_2 efflux for 2011 and 2012, respectively, from the linear relationships, demonstrating that soil temperature is a significant factor in driving CO_2 efflux in the dominated tundra plants during the growing season. The Q_{10} value for soil temperature at 5 cm depth for the moss regime in August 2012 was the lowest at 1.15, resulting from higher soil temperature and higher soil moisture in August 2012 (Table 1).

Figure 5 shows the responses of monthly averaged CO_2 efflux to soil temperature at 5 and 10 cm depths (Fig. 5a1 and b1), soil moisture (Fig. 5a2 and b2), and thaw depth (Fig. 5a3 and b3), and the responses of soil temperature at 5 cm to soil moisture (Fig. 5a4 and b4) and thaw depth (Fig. 5a5 and b5) during the growing seasons of 2011 and 2012. Except for Fig. 5a1 and b1, the relationship between both was related negatively during the growing season of 2011–12. However, except for data measured in September 2012, the relationships between both components denote positive lines from June to August 2012, as also shown in Fig. 5b2–b5. This seems to be the effect of heavy rainfall since 20 August 2012, as shown in Fig. 6, which represents daily and accumulative precipitation in 2011 and 2012. Interestingly, the accumulative rainfall began to surpass 2011 accumulative precipitation since 20 August 2012. The correlation coefficient (R^2) from June to August 2012 ranged from 0.01 in Fig. 5b3 to 0.32 in Fig. 5b2. Hence, soil moisture elucidated 32 % of the variability in CO_2 efflux before the severe rainfall event of the fall season of 2012, demonstrating that soil moisture is another important factor, next to soil temperature. Jensen et al. (2014) estimated 2.3 ± 0.2 and 1.3 ± 0.11 mg CO_2 m^{-2} min^{-1} in the northwestern tundra of Alaska in July of 2011 and 2012, respectively, suggesting the lower carbon flux results from the stronger rainfall event in 2012 (Jensen et al., 2014: see Fig. 3a), with a similar trend in air temperature between both years. This rainfall may have possibly inhibited 43 % of CO_2 emission from the soil surface with increasing soil moisture in 2012, indicating a similar result to that observed in this study (Davidson et al., 1998).

3.3 Simulated CO_2 efflux from a Hierarchical Bayesian model

We used 486 datasets of CO_2 efflux, soil temperature, soil moisture, vegetation types, and thaw depth for adjusting the parameters of a hierarchical Bayesian (HB) model, and the posterior distribution of the parameter for the CO_2 efflux are summarized in Table 3. Potential CO_2 effluxes from the dominated plants calculated from posterior medians of the model were 16.8 mg CO_2 m^{-2} min^{-1} in grass (95 % predicted credible intervals (CI), 13.7–20.4 mg CO_2 m^{-2} min^{-1}), 15.3 mg CO_2 m^{-2} min^{-1} in lichen (95 % predicted CI, 11.1–16.8 mg $CO_2 m^{-2}$ min^{-1}), 14.8 mg CO_2 m^{-2} min^{-1} in moss (95 % predicted CI, 10.2–15.9 mg CO_2 m^{-2} min^{-1}), and 21.9 mg CO_2 m^{-2} min^{-1} in tussock (95 % predicted CI, 24.0–31.0 mg CO_2 m^{-2} min^{-1}). This suggests that the contribution of atmospheric carbon from tussock tundra should receive attention when it comes to the tundra ecosystem and a circumpolar scale response to the changing climate in the higher Northern Hemisphere (Oechel et al., 1997; Bhatt et al., 2010, 2013; Kim et al., 2013).

BGD
11, 5903–5939, 2014

We computed the limiting functions for soil temperature, soil moisture, and thaw depth of CO_2 efflux simulated by posterior distributions ($n = 1000$), as shown in Fig. 7, for the quantitative assessment of the driving parameters on CO_2 efflux. For soil temperature limiting functions, the factor simulated from the posterior median followed soil temperature nearly exponentially (Fig. 7a), demonstrating the definite temperature dependency of CO_2 efflux (Raich and Schlesinger, 1992; Davidson et al., 1998; Gaumont-Guay et al., 2006; Mahecha et al., 2010; Kim et al., 2013), as shown in Fig. 5a1 and b1. For soil temperature response, the parameter Q_{10} value was 2.52 ± 0.12 (95 % predicted CI, 2.29–2.75). For soil moisture limiting functions (Fig. 7b), optimum soil moisture value was 0.228 $m^3 m^{-3}$ (95 % predicted CI, 0.184–0.238 $m^3 m^{-3}$). CO_2 efflux tended to increase with the increase in soil moisture, when the soil moisture value was to the optimum, as shown in Figs. 5a2 and b2. On the other hand, the response from CO_2 efflux to soil moisture changed to a negative trend beyond the optimum value of soil moisture. The results from Jensen et al. (2014) proved the findings observed in this study, in which CO_2 efflux was relatively lower with the higher soil moisture observed in 2012, compared to 2011 (Jensen et al., 2014: see Fig. 4b). Davidson et al. (1998) reported the correlation of soil water content and CO_2 efflux in different drainage classes. CO_2 efflux increased when soil water content was less than 0.2 $m^3 m^{-3}$; on the other hand, higher soil moisture resulted in a decrease in CO_2 efflux (Davidson et al., 1998: see Fig. 7). For thaw depth limiting functions, the factor increased to 20 cm, which is the optimum thaw depth value (Fig. 7c). While CO_2 efflux increased with the rise in thaw depth in June until the optimum thaw depth value, efflux was constant, despite an increase in thaw depth with time. The response of CO_2 efflux on thaw depth turned to a negative trend during the growing seasons of 2011 and 2012, as shown in Fig. 5a3 and b3. These findings suggest that thaw depth may be not a significant factor in influencing CO_2 efflux in the tundra ecosystem, in spite of a deeper active layer over time.

Figure 8 shows the spatial distribution of simulated CO_2 efflux calculated from the posterior medians of the hierarchical Bayesian model during the growing seasons of

BGD
11, 5903–5939, 2014

2011 and 2012, excluding July and September of 2011. The pattern of simulated CO_2 efflux is nearly identical to the spatial distribution of measured CO_2 efflux (Fig. 5), as simulated CO_2 efflux is a function of soil temperature, soil moisture, and thaw depth. Of these, we consider soil temperature the most important parameter in modulating CO_2 efflux in the tundra ecosystem during the growing season. We compared measured CO_2 efflux with predicted CO_2 efflux using posterior medians in the HB model at each sampling period of 2011 and 2012 (Fig. 9), denoting that CO_2 efflux simulated by a nonlinear equation is consistent with measured data. Using the HB model, accumulative predicted CO_2 emission rates from 28 June to 30 September of 2011 and 2012, based on monitored soil temperature and soil moisture in the Council area, were 742 g CO_2 m^{-2} $period^{-1}$ (95 % predicted CI, 646–839 g CO_2 m^{-2} $period^{-1}$) and 539 g CO_2 m^{-2} $period^{-1}$ (95 % predicted CI, 460–613 g CO_2 m^{-2} $period^{-1}$), respectively. These findings suggest that the 2012 CO_2 emission rate is constrained by 27 % (95 % CI, 17–36 %) compared to the 2011 emission, demonstrating that higher soil moisture from severe rain constrains the emission of soil-produced CO_2 to the atmosphere (Jensen et al., 2014).

During the study periods (DOY: 179–273; Fig. 10) of 2011 and 2012, average soil temperature was 9.3 ± 3.8 (CV: 41 %) and 8.6 ± 4.8 (CV: 56 %) °C, respectively, showing that there is no significant difference between the years, based on a one-way ANOVA 95 % confidence level. Trends in soil temperature during the periods of 2011 and 2012 were $ST = -0.135 \times DOY + 5522$ ($R^2 = 0.70$), and $ST = -0.093 \times DOY + 3781$ ($R^2 = 0.45$), respectively; on the other hand, trends for soil moisture were $SM = 0.0025 \times DOY - 103.5$ ($R^2 = 0.37$) in 2011, and $SM = -0.0008 \times DOY + 33.2$ ($R^2 = 0.31$) in 2012, as shown in Fig. 10. Average soil moisture was 0.260 ± 0.040 (15 %) and 0.493 ± 0.124 (25 %) $m^3\,m^{-3}$ in 2011 and 2012, respectively, suggesting a distinct difference in soil moisture between both years. Soil moisture during the 2012 period did not change with time, resulting from heavy rainfall events (Figs. 1 and 6) during the growing season (Jensen et al., 2014). When the soil temperature at the end of September in 2012 was below zero (Fig. 10a), soil moisture sharply decreased, suggesting the frozen layer reached to the measuring depth (e.g., near surface) of soil moisture, as shown in Fig. 10b. The case of 2012 weather conditions may be an episodic event, needing additional monitoring for several representative points within the plot. Nevertheless, the higher CO_2 emission rate in 2011 simulated by the HB model is thought likely to be the result of CO_2 efflux increases until soil moisture reached to optimum value, as shown in Fig. 7b. Therefore, soil moisture plays an important parameter in constraining CO_2 emission in this tundra ecosystem when the soil moisture is over the optimum value. When the annual simulated CO_2 emission rate was estimated from the relationship between CO_2 efflux and air temperature using the Eq. (2), the annual emission rates were 862 and 670 g CO_2 m^{-2} $year^{-1}$ in 2011 and 2012, respectively, corresponding to 86 and 80 % of annual CO_2 emission rates. Kim et al. (2013) estimated growing season CO_2 emission in the foothill tundra north of Brooks Range, Alaska was 645 g CO_2 m^{-2} $period^{-1}$ during 2006–2010, despite the difference in latitudinal distributions for CO_2 efflux and environmental parameter. This value is situated between the 2011 and 2012 emission rates simulated in Council in this study. That is, the simulated CO_2 emission rates were 0.86–1.20 Mg CO_2 $period^{-1}$ within a 40 m × 40 m plot during the growing seasons of 2012 and 2011, respectively.

4 Summary and future works

Here, CO_2 efflux-measurement with a manual chamber system was conducted in the tundra ecosystem of the Seward Peninsula of western Alaska during the growing seasons of 2011 and 2012, for what is (are) significant parameter(s) in controlling CO_2 efflux, and the effect(s) on the soil-produced CO_2 emission rate to the atmosphere, using a hierarchical Bayesian (HB) model within a 40 m × 40 m plot (5 m interval; 81 points). Tussock tundra is an atmospheric carbon source in the tundra ecosystem year-round (Oechel et al., 1997; Kim et al., 2007, 2013). Considering the wide-ranged distribution of tussock in the high Northern Hemisphere, tussock- and moss-originated CO_2 efflux measurement should not be overlooked as a significant carbon source in estimating regional and global carbon budget. Response of CO_2 efflux in tussock on soil temperature denoted a linear relationship; on the other hand, effluxes observed in lichen and moss regimes increased exponentially as soil temperature increased. This finding suggests that soil temperature is an environmental parameter in modulating CO_2 efflux, as many scientists have reported around the world. Except for data observed in September 2012, soil moisture played an important parameter in controlling CO_2 efflux. For 2012, higher soil moisture, resulting from the heavy rainfall in the end of August, was a constraining factor the transport of soil-produced carbon to the atmosphere (Davidson et al., 1998; Jensen et al., 2014).

Using a HB model, we computed the limiting functions to soil temperature, soil moisture, and thaw depth of CO_2 efflux simulated by the posterior distribution. Simulated CO_2 efflux increased (1) exponentially as soil temperature increased and (2) nearly linearly until soil moisture was an optimum values ($0.228\,m^3\,m^{-3}$); however, efflux decreased logarithmically when soil moisture was beyond the optimum, and (3) nearly linearly until thaw depth was at optimum value (20 cm); finally, efflux stayed constant when thaw depth increased with time. These simulated findings show similar patterns to the data obtained in this study as well as to Jensen et al. (2014)'s results, observed in the northwestern tundra of Alaska during the growing seasons of 2011 and 2012. During these growing seasons of 2011 and 2012, the difference in soil temperature between both years was not significant; however, there was a distinct difference in soil moisture between the two, resulting in the inhibition of CO_2 emissions due to higher soil moisture. This demonstrates that higher soil moisture is constrained to 27 % of CO_2 emission in 2012 rather than 2011. However, to prove the effect of soil moisture on controlling CO_2 emission in the tundra ecosystem, additional study must monitor the profiles of soil moisture and soil temperature at representative points from lichen, moss, and tussock tundra regimes within the plot. As conducted by Risk et al. (2011), the monitoring of soil CO_2 efflux must also show representative points along with the monitoring of environmental parameter profiles within the plot.

BGD
11, 5903–5939, 2014

Supplementary material related to this article is available online at http://www.biogeosciences-discuss.net/11/5903/2014/bgd-11-5903-2014-supplement.pdf.

Acknowledgements. This work was supported by the National Research Foundation of Korea Grant funded by the Korean Government (MSIP) (NRF-C1ABA001-2011-0021063) (Title: Establishment of Circum-Arctic Permafrost Environment Change Monitoring Network and Future Prediction Techniques (CAPEC Project)). This research was conducted under the JAMSTEC-IARC Collaboration Study with funding provided by the Japan Agency for Marine-Earth Science and Technology (JAMSTEC), and the IARC–JAXA Information System (IJIS) with funding partly provided by the Japan Aerospace Exploration Agency (JAXA) under a grant to the International Arctic Research Center (IARC).

References

ACIA (Arctic Climate Impact Assessment): Impacts of a Warming Arctic, Cambridge Univ. Press, Cambridge, UK, 146 pp, 2004.

Bhatt, U. S., Walker, D. A., Raynolds, M. K., Comiso, J. C., Epstein, H. E., Jia, G., Gens, R., Pinzon, J. E., Tucker, C. J., Tweedie, C. E., and Webber, P. J.: Circumpolar arctic tundra vegetation change is linked to sea ice decline, Earth Interact., 14, 1–20, doi:10.1175/2010EI315.1, 2010.

Bhatt, U. S., Walker, D. A., Raynolds, M. K., Bieniek, P. A., Epstein, H. E., Comis, J. C., Pinzon, J. E., Tucker, C. J., and Polyako, I. V.: Recent declines in warming and vegetation greening trends over pan-Arctic tundra, Remote Sens., 5, 4229–4254, doi:10.3390/rs5094229, 2013.

Bond-Lamberty, B. and Thomson, A.: Temperature-associated increases in the global soil respiration record, Nature, 464, 597–582, 2010.

Clark, J. S.: Why environmental scientists are becoming Bayesians, Ecol. Lett., 8, 2–14, doi:10.1111/j.1461-0248.2004.00702.x, 2005.

Davidson, E. A. and Janssens, I. A.: Temperature sensitivity of soil carbon decomposition and feedback to climate change, Nature, 440, 165–173, 2006.

Davidson, E. A., Belk, E., and Boone, R. D.: Soil water content and temperature as independent or confounded factors controlling soil respiration in a temperate mixed hardwood forest, Glob. Change Biol., 4, 217–227, 1998.
Davidson, E. A., Savage, K., Verchot, L. V., and Bavarri, R.: Minimizing artifacts and biases in chamber-based measurements of soil respiration, Agr. Forest Meteorol., 113, 21–37, 2002.
Elberling, B., Michelsen, A., Schädel, C., Schuur, E. A. G., Christiansen, H. H., Berg, L., Tamstorf, M., and Sigsgaard, C.: Long-term CO_2 production flowing permafrost thaw, Nat. Clim. Change, 3, 890–894, doi:10.1038/NCLIMATE1955, 2013.
Gaumont-Guay, D., Black, T. A., Griffis, T. J., Barr, A. G., Jassal, R. A., and Nesic, Z.: Interpreting the dependence of soil respiration on soil temperature and water content in a boreal aspen stand, Agr. Forest Meteorol., 140, 220–235, 2006.
Grosse, G., Harden, J., Turetsky, M., McGuire, A. D., Camill, P., Tarnocai, C., Frolking, S., Schuur, E. A. G., Jorgenson, T., Marchenko, S., Romanovsky, V., Wickland, K. P., French, N., Waldrop, M., Bourgeau-Chaves, L., and Striegl, R. G.: Vulnerability of high-latitude soil organic carbon in North America to disturbance, J. Geophys. Res., 116, G00K06, doi:10.1029/2010JG001507, 2011.
Hinzman, L. D., Bettez, N. D., Bolton, W. R., Chapin, F. S., Dyurgerov, M. B., Fastie, C. L., Griffith, B., Hollister, R. D., Hope, A., Huntington, H. P., Jensen, A. M., Jia, G. J., Jorgenson, T., Kane, D. L., Klein, D. R., Kofinas, G., Lynch, A. H., Lloyd, A. H., McGuire, A. D., Nelson, F. E., Oechel, W. C., Osterkamp, T. E., Racine, C. H., Romanovsky, V. E., Stone, R. S., Stow, D. A., Sturm, M., Tweedie, C. E., Vourlitis, G. L., Walker, M. D., Walker, D. A., Webber, P. J., Welker, J. M., Winker, K. S., and Yoshikawa, K.: Evidence and implications of recent climate change in northern Alaska and other arctic regions, Climatic Change, 72, 251–298, 2005.
Hutchinson, G. L. and Livingston, P.: Soil-atmosphere gas exchange, in: Methods of Soil Analysis: Part 4, Physical Methods, 3rd ed., edited by: Dane, J. H. and Topp, G. C., SSSA Book Series 5, Madison, WI, Soil Sci. Soc. Am. J., 1159–1182, 2002.
Jensen, A. E., Lohse, K. A., Crosby, B. T., and Mora, C. I.: Variations in soil carbon dioxide efflux across a thaw slump chronosequence in northwestern Alaska, Environ. Res. Lett., 9, 025001, doi:10.1088/1748-9326/9/2/025001, 2014.
Kim, Y., Ueyama, M., Nakagawa, F., Tsunogai, U., Tanaka, N., and Harazono, Y.: Assessment of winter fluxes of CO_2 and CH_4 in boreal forest soils of central Alaska estimated by the

BGD
11, 5903–5939, 2014

Constraint of soil moisture on CO_2 efflux in tundra ecosystem

Y. Kim et al.

profile method and the chamber method: a diagnosis of methane emission and implications for the regional carbon budget, Tellus B, 59, 223–233, 2007.
Kim, Y., Kim, S. D., Enomoto, H., Kushida, K., Kondoh, M., and Uchida, M.: Latitudinal distribution of soil CO_2 efflux and temperature along the Dalton Highway, Alaska, Polar Sci., 7, 162–173, 2013.
Koven, C. D., Ringeval, B., Friedlingstein, P., Ciais, P., Cadule, P., Khvorostyanov, D., Krinner, G., and Tarnocai, C.: Permafrost carbon-climate feedbacks accelerate global warming, P. Natl. Acad. Sci. USA, 108, 14769–14774, 2011.
Lloyd, J. and Taylor, J. A.: On the temperature dependence of soil respiration, Funct. Ecol., 8, 315–323, 1994.
Mahecha, M. D., Reichstein, M., Carvalhais, N., Lasslop, G., Lange, H., Seneviratne, S. I., Vargas, R., Ammann, C., Arain, M. A., Cescatti, A., Janssens, I. A., Migliavacca, M., Montagnani, L., and Richardson, A. D.: Global convergence in the temperature sensitivity of respiration at ecosystem level, Science, 329, 838–840, 2010.
Malcom, G. M., López-Gutiérres, J., and Koide, R. T.: Temperature sensitivity of respiration differs among forest floor layers in a *Pinus resinosa* plantation, Soil Biol. Biochem., 41, 1075–1079, 2009.
Marchenko, S., Romanovsky, V., and Tipenko, G.: Numerical modeling of spatial permafrost dynamics in Alaska, in: Proceedings of the Ninth International Conference on Permafrost, edited by Kane, D. L., and Hinkel, K. M., Inst. of North. Eng., Univ. of Alaska Fairbanks, Fairbanks, 1125–1130, 2008.
Michaelson, G. J. and Ping, C. L.: Soil organic carbon and CO_2 respiration at subzero temperature in soils of Arctic Alaska, J. Geophys. Res., 108, 8164, doi:10.1029/2001JD000920, 2003.
Miller, P. C., Kendall, R., and Oechel, W. C.: Simulating carbon accumulation in northern ecosystems, Simulation, 40, 119–131, 1983.
Monson, R. K., Lipson, D. L., Burns, S. P., Turnipseed, A. A., Delany, A. C., Williams, M. W., and Schmidt, S. K.: Winter forest soil respiration controlled by climate and microbial community composition, Nature, 439, 711–714, doi:10.1038/nature04555, 2006.
Nishina, K., Takenaka, C., and Ishizuka, S.: Spatial variations in nitrous oxide and nitric oxide emission potential on a slope of Japanese ceder (*Cryptomeria japonica*) forest, Biogeochemistry, 96, 163–175, 2009.

Nishina, K., Akiyama, H. Nishimura, S., Sudo, S., and Yagi, K.: Evaluation of uncertainties in N_2O and NO fluxes from agricultural soil using a Hierarchical Bayesian model, J. Geophys. Res., 117, G04008, doi:10.1029/2012JG002157, 2012.

Oberbauer, S. F., Tweedie, C. E., Welker. J. M., Fahnestock, J. T., Henry, G. H. R., Webber, P. J., Hillister, R. D., Waler, M. D., Kuchy, A., Elmore, E., and Starr, G.: Tundra CO_2 fluxes in response to experimental warming across latitudinal and moisture gradients, Ecol. Monogr., 72, 221–238, 2007.

Oechel, W. C., Vourlitis, G., and Hastings, S. J.: Cold season CO_2 emissions from arctic soils, Global Biogeochem. Cy., 11, 163–172, 1997.

Oechel, W. C., Vourlitis, G., Hastings, S. J., Zulueta, R. C., Hinzman, L. D., and Kane, D.: Acclimation of ecosystem CO_2 exchange in the Alaska Arctic in response to decadal climate warming, Nature, 406, 978–981, 2000.

Ping, C. L., Michaelson, G. J., Jorgenson, M. T., Kimble, J. H., Epstein, H., Romanovsky, V., and Walker, D. A.: High stock of soil organic carbon in the North American Arctic region, Nat. Geosci., 1, 615–619, doi:10.1038/ngeo284, 2008.

Poole, K. D. and Miller, P. C.: Carbon dioxide flux from three Arctic tundra types in North-Central Alaska, USA, Arctic Alpine Res., 14, 27–32, 1982.

Post, E., Bhatt, U. S., Bitz, C. M., Brodie, J., Fulton, T. L., Hebblewhite, M., Kerby, J., Kutz, S., Stirling, J. K., and Walker, D. A.: Ecological consequences of sea-ice decline, Science, 341, 519, doi:10.1126/science.1235225, 2013.

R Development Core Team: R: a Language and Environment for Statistical Computing, R Found. Comput., Vienna, available at: http://www.R-project.org/, 2012.

Raich, J. W. and Schlesinger, W. H.: The global carbon dioxide flux in soil respiration and its relationship to vegetation and climate, Tellus B, 44, 81–99, 1992.

Rayment, M. B. and Jarvis, P. G.: Temporal and spatial variation of soil CO_2 efflux in a Canadian boreal forest, Soil Biol. Biochem., 32, 35–45, 2000.

Risk, D., Nickerson, N., Creelman, C., McArthur, G., and Owens, J.: Forced diffusion soil flux: a new technique for continuous monitoring of soil gas efflux, Agr. Forest Meteorol., 151, 1622–1631, 2011.

Romanovsky, V., Burgess, M., Smith, S., Yoshikawa, K., and Brown, J.: Permafrost temperature records: indicators of climate change, EOS Trans. AGU, 80, 589–594, doi:10.1029/2002EO000402, 2002.

BGD
11, 5903–5939, 2014

Savage, K. E. and Davidson, E. A.: A comparison of manual and automated systems for soil CO_2 flux measurements: trade-offs between spatial and temporal resolution, J. Exp. Bot., 54, 891–899, 2003.

Schlesinger, W. H. and Andrews, J. A.: Soil respiration and the global carbon cycle, Biogeochemistry, 48, 7–20, 2000.

Schuur, E. A. G., Vogel, J. G., Crummer, K. G., Lee, H., Sickman, J. O., and Osterkamp, T. E.: The effect of permafrost thaw on old carbon release and net carbon exchange from tundra, Nature, 459, 556–559, doi:10.1038/nature0803, 2009.

Smith, L. C., Sheng, Y., MacDonal, G. M., and Hinzman, L. D.: Disappearing Arctic lakes, Science, 308, 1429, doi:10.1126/science.1108142, 2005.

Spiegelhalter, D. T. A. and Best, N.: WinBUGS User Manual, MRC Biostatistics Unit, Cambridge, UK, 2000.

Sturm, M., J. Schimel, J., Michaelson, G., Welker, J. M., Oberbauer, S. F., Liston, G. E., Fahnestock, J., and Romanovsky, V.: Winter biological processes could help convert Arctic tundra to shrubland, Bioscience, 55, 17–26, 2005.

Tarnocai, C., Canadell, J. G., Schuur, E. A. G., Kuhry, P., Mazhitova, G., and Zimov, S.: Soil organic carbon pools in the northern circumpolar permafrost region, Global Biogeochem. Cy., 23, GB2023, doi:10.1029/2008GB003327, 2009.

Walker, D. A., Auerbach, N. A., Bockheim, J. G., Chapin III, F. S., Eugster, W., King, J. Y., McFadden, J. P., Michaelson, G. J., Nelson, F. E., Oechel, W. C., Ping, C. L., Reeburg, W. S., Regli, S., Shiklomanov, N. I., and Vourlitis, G. L.: Energy and trace-gas fluxes across a soil pH boundary in the Arctic, Nature, 394, 469–472, 1998.

Walter, K. M., Smith, L. C., and Chapin, F. S.: Methane bubbling from northern lakes: present and future contributions to the global methane budget, Philos. T. R. Soc. A, 365, 1657–1676, 2007.

Whalen, S. C. and Reeburgh, W. S.: A methane flux time series for tundra environments, Global Biogeochem. Cy., 5, 261–273, 1988.

Xu, M. and Qi, Y.: Soil-surface CO_2 efflux and its spatial and temporal variations in a young ponderosa pine plantation in northern California, Glob. Change Biol., 7, 667–677, 2001.

Yoshikawa, K. and Hinzman, L. D.: Shrinking thermokarst ponds and groundwater dynamics in discontinuous permafrost near Council, Alaska, Permafrost Periglac., 14, 151–160, 2003.

BGD

11, 5903–5939, 2014

Constraint of soil moisture on CO_2 efflux in tundra ecosystem

Y. Kim et al.

Table 1. Average ± standard deviation (coefficient of variation, %) of CO_2 efflux, soil temperature at 5 and 10 cm below the surface, soil moisture, thaw depth, and pH in lichen, moss, and tussock tundra, Council, Seward Peninsula, Alaska during growing seasons of 2011 and 2012.

Month	Vegetation	n	CO_2 efflux	Soil temperature (°C)		Soil moisture	Thaw depth	pH
			($mg\,CO_2\,m^{-2}\,min^{-1}$)	5 cm	10 cm	($m^3\,m^{-3}$)	(cm)	
Jun, 2011	Lichen	22	5.7 ± 3.6 (63)	10.1 ± 2.5 (25)	3.3 ± 1.4 (42)	0.270 ± 0.162 (60)	22 ± 3 (12)	n.m.[c]
	Moss	43	7.8 ± 2.2 (29)	13.2 ± 2.9 (22)	6.7 ± 2.8 (42)	0.224 ± 0.122 (54)	21 ± 3 (14)	n.m.
	Tussock	16	12.9 ± 6.2 (48)	12.7 ± 3.3 (26)	7.6 ± 3.7 (48)	0.301 ± 0.116 (39)	22 ± 2 (11)	n.m.
	Average	81[a]	8.0 ± 3.6 (45)	12.3 ± 3.2 (53)	6.0 ± 3.1 (51)	0.255 ± 0.127 (49)	21 ± 3 (14)	
Aug, 2011	Lichen	24	2.5 ± 1.2 (47)	6.9 ± 1.5 (22)	4.4 ± 1.1 (25)	0.297 ± 0.200 (67)	38 ± 5 (14)	n.m.
	Moss	41	3.3 ± 1.7 (52)	9.0 ± 1.6 (18)	6.2 ± 1.7 (27)	0.264 ± 0.237 (90)	41 ± 8 (19)	n.m.
	Tussock	16	5.1 ± 2.7 (53)	9.4 ± 2.4 (25)	7.0 ± 2.1 (30)	0.256 ± 0.141 (55)	40 ± 5 (12)	n.m.
	Average	81[a]	3.3 ± 1.3 (39)	8.6 ± 1.9 (22)	5.8 ± 1.4 (24)	0.272 ± 0.180 (66)	40 ± 6 (15)	
Sep, 2011	Lichen	23	2.3 ± 0.9 (40)	6.2 ± 1.0 (16)	4.6 ± 1.0 (21)	–[b]	57 ± 8 (13)	3.7 ± 0.4 (7)
	Moss	43	2.5 ± 1.2 (50)	6.9 ± 1.4 (20)	5.6 ± 1.3 (23)	–	58 ± 12 (20)	3.8 ± 0.4 (11)
	Tussock	15	3.5 ± 1.5 (43)	6.5 ± 1.4 (22)	5.2 ± 1.3 (25)	–	55 ± 5 (8)	3.8 ± 0.3 (8)
	Average	81[a]	2.6 ± 0.8 (30)	6.0 ± 1.6 (26)	5.3 ± 1.1 (21)	–	57 ± 9 (16)	3.8 ± 0.4 (11)
Jun, 2012	Lichen	25	3.7 ± 2.0 (53)	11.1 ± 3.0 (27)	5.9 ± 2.6 (44)	0.213 ± 0.113 (53)	22 ± 3 (12)	–[b]
	Moss	38	4.7 ± 1.8 (39)	12.7 ± 2.4 (19)	7.1 ± 2.3 (32)	0.189 ± 0.097 (51)	21 ± 3 (16)	–
	Tussock	14	5.6 ± 1.9 (33)	12.2 ± 2.4 (19)	8.8 ± 2.5 (29)	0.339 ± 0.136 (40)	21 ± 2 (11)	–
	Grass	4	5.2 ± 2.1 (40)	10.4 ± 3.0 (28)	6.4 ± 2.1 (33)	0.304 ± 0.149 (49)	21 ± 2 (8)	–
	Average	81[a]	4.8 ± 2.0 (42)	11.5 ± 2.6 (23)	6.6 ± 2.5 (38)	0.224 ± 0.125 (56)	21 ± 3 (14)	
Jul, 2012	Lichen	25	4.0 ± 1.5 (38)	10.1 ± 2.1 (21)	6.9 ± 1.8 (26)	0.165 ± 0.088 (53)	33 ± 3 (9)	–[b]
	Moss	38	4.3 ± 1.5 (35)	11.2 ± 2.4 (22)	7.9 ± 1.9 (25)	0.243 ± 0.086 (60)	31 ± 4 (13)	–
	Tussock	14	5.9 ± 2.8 (48)	10.5 ± 2.5 (23)	7.9 ± 2.5 (31)	0.268 ± 0.140 (52)	31 ± 2 (8)	–
	Grass	4	5.6 ± 1.9 (34)	9.9 ± 1.1 (11)	6.6 ± 1.0 (15)	0.208 ± 0.088 (42)	36 ± 6 (16)	–
	Average	81[a]	5.0 ± 2.0 (40)	11.3 ± 2.2 (19)	7.2 ± 2.4 (33)	0.191 ± 0.118 (62)	33 ± 6 (18)	
Aug, 2012	Lichen	25	3.3 ± 1.1 (33)	13.0 ± 2.6 (20)	9.3 ± 2.2 (23)	0.201 ± 0.117 (58)	45 ± 4 (10)	–[b]
	Moss	38	4.7 ± 1.6 (35)	16.0 ± 2.5 (15)	11.9 ± 2.7 (22)	0.258 ± 0.115 (73)	44 ± 7 (15)	–
	Tussock	14	6.4 ± 2.1 (33)	16.2 ± 2.5 (15)	12.6 ± 4.0 (32)	0.288 ± 0.120 (42)	43 ± 3 (7)	–
	Grass	4	5.5 ± 2.4 (43)	13.2 ± 0.8 (6)	9.3 ± 1.2 (13)	0.199 ± 0.069 (35)	47 ± 11 (22)	–
	Average	81[a]	4.8 ± 1.9 (40)	15.0 ± 2.9 (19)	11.0 ± 3.2 (29)	0.246 ± 0.126 (51)	45 ± 6 (13)	
Sep, 2012	Lichen	25	1.6 ± 0.9 (54)	3.5 ± 1.9 (55)	2.1 ± 1.6 (75)	0.465 ± 0.260 (56)	59 ± 7 (11)	–[b]
	Moss	38	1.8 ± 0.8 (44)	4.9 ± 2.3 (47)	3.1 ± 1.8 (59)	0.340 ± 0.264 (78)	60 ± 9 (16)	–
	Tussock	14	2.3 ± 1.0 (44)	5.9 ± 2.5 (42)	4.1 ± 2.0 (48)	0.427 ± 0.121 (28)	57 ± 4 (7)	–
	Grass	4	2.2 ± 0.9 (40)	2.9 ± 2.5 (26)	2.0 ± 1.6 (82)	0.456 ± 0.378 (82)	64 ± 9 (14)	–
	Average	81[a]	1.9 ± 0.8 (42)	4.4 ± 2.2 (50)	2.7 ± 1.8 (65)	0.424 ± 0.262 (62)	60 ± 8 (13)	

[a] denots total measured points.
[b] – is not conducted.
[c] n.m. indicates not measured.

BGD
11, 5903–5939, 2014

Constraint of soil moisture on CO_2 efflux in tundra ecosystem

Y. Kim et al.

Table 2. Q_{10} values and correlation coefficient between CO_2 efflux and soil temperature at 5 and 10 cm below the soil surface in lichen, moss, and tussock during the growing season based on a one-way ANOVA with a 95 % confidence level.

Vegetation, Year	Month	5 cm			10 cm		
		Q_{10}	R^2	p	Q_{10}	R^2	p
Lichen, 2011	Jun	2.05	0.10	< 0.001	1.68	0.01	0.018
	Aug	8.58	0.36	< 0.001	2.47	0.04	< 0.001
	Sep	10.59	0.43	< 0.001	6.87	0.32	< 0.001
	Total	4.97	0.34	< 0.001	1.06	0.01	0.032
Moss, 2011	Jun	1.58	0.26	< 0.001	1.54	0.15	0.073
	Aug	6.59	0.40	< 0.001	5.88	0.41	< 0.001
	Sep	7.54	0.28	< 0.001	10.10	0.78	< 0.001
	Total	5.05	0.62	< 0.002	4.46	0.21	< 0.001
Tussock, 2011	Jun	2.68	0.54	0.890	2.01	0.33	0.005
	Aug	8.66	0.68	< 0.001	11.70	0.66	0.041
	Sep	10.74	0.58	< 0.001	9.64	0.44	0.008
	Total	6.15	0.73	0.018	5.44	0.39	0.467
Lichen, 2012	Jun	4.03	0.66	< 0.001	1.40	0.24	< 0.001
	Jul	5.04	0.69	< 0.001	0.57	0.65	< 0.001
	Aug	2.41	0.46	< 0.001	2.50	0.35	< 0.001
	Sep	6.17	0.57	< 0.001	9.55	0.59	< 0.001
	Total	2.86	0.65	< 0.001	1.09	0.19	< 0.001
Moss, 2012	Jun	2.62	0.37	< 0.001	0.95	0.01	< 0.001
	Jul	3.82	0.66	< 0.001	3.51	0.51	< 0.001
	Aug	1.15	0.01	< 0.001	1.14	0.01	< 0.001
	Sep	2.10	0.16	< 0.001	2.18	0.11	< 0.001
	Total	2.44	0.54	< 0.001	2.35	0.33	< 0.001
Tussock, 2012	Jun	5.06	0.77	< 0.001	4.59	0.68	< 0.001
	Jul	3.78	0.73	< 0.001	2.78	0.50	< 0.001
	Aug	2.98	0.77	< 0.001	1.59	0.37	< 0.001
	Sep	4.12	0.72	< 0.001	5.01	0.59	< 0.001
	Total	3.11	0.76	< 0.001	3.00	0.62	< 0.001
Grass, 2012	Total	2.28	0.41	< 0.001	3.11	0.38	< 0.001

BGD
11, 5903–5939, 2014

Table 3. Summary of the posterior distribution fro each parameter.

Parameter	Mean	S.D.	2.5 %	97.5 %	Rhat
β_0	16.55	3.975	8.393	23.837	1.006
Q_{10}	2.517	0.115	2.291	2.752	1.009
a	−1.276	0.476	−1.966	−0.312	1.003
b	0.249	0.111	0.105	0.483	1.003
c	2.043	0.573	1.054	2.956	1.001
d	3.657	2.816	0.098	9.460	1.006
k	4.973	2.900	0.287	9.722	1.001
r	0.511	0.289	0.025	0.976	1.003
τ_{vege}	0.176	0.126	0.024	0.501	1.007
τ_{year}	0.072	0.059	0.006	0.226	1.006
τ^*	0.225	0.013	0.199	0.252	1.001
deviance	2470.946	4.215	2464.93	2480.98	1.001

* τ indicates $1/\sigma$.

BGD
11, 5903–5939, 2014

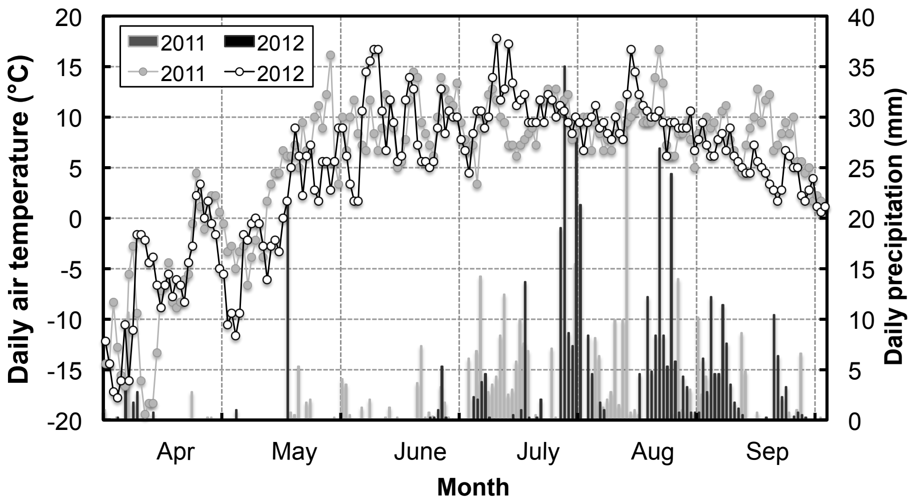

Fig. 1. Average daily ambient temperature and precipitation in Council, Seward Peninsula, Alaska during April–October of 2011 and 2012 (Western Regional Climate Center).

BGD
11, 5903–5939, 2014

Constraint of soil moisture on CO_2 efflux in tundra ecosystem

Y. Kim et al.

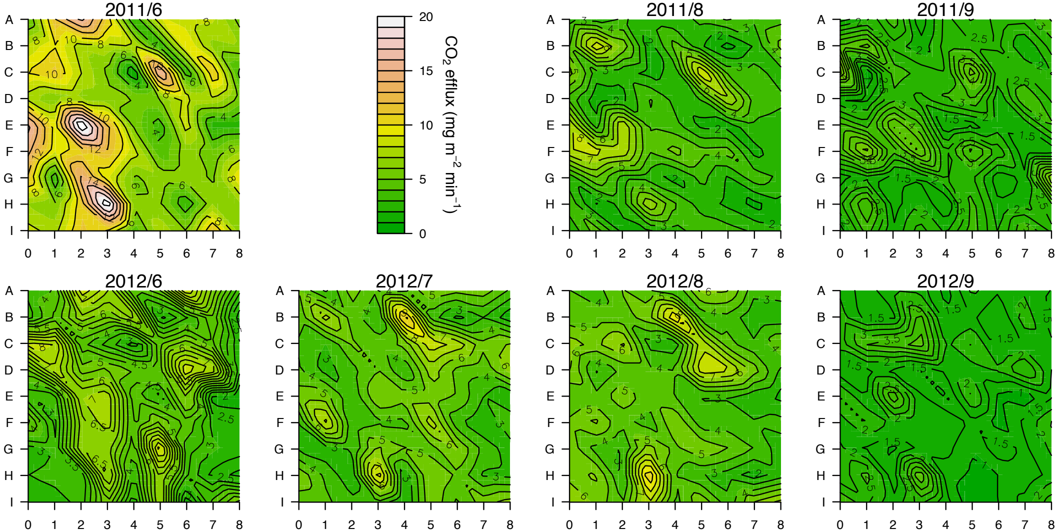

Fig. 2. Spatial distribution of CO_2 efflux (mg CO_2 m^{-2} min^{-1}) within a 40 m × 40 m plot (5 m interval; 81 points), Council, Seward Peninsula, Alaska during the growing seasons of 2011 (upper panel) and 2012 (lower). Due to the heavy rain in early July 2011, this data could not be measured, as shown in Fig. 1.

BGD
11, 5903–5939, 2014

BGD
11, 5903–5939, 2014

Constraint of soil moisture on CO_2 efflux in tundra ecosystem

Y. Kim et al.

Title Page
Abstract | Introduction
Conclusions | References
Tables | Figures
◀| |▶
◀ ▶
Back | Close
Full Screen / Esc
Printer-friendly Version
Interactive Discussion

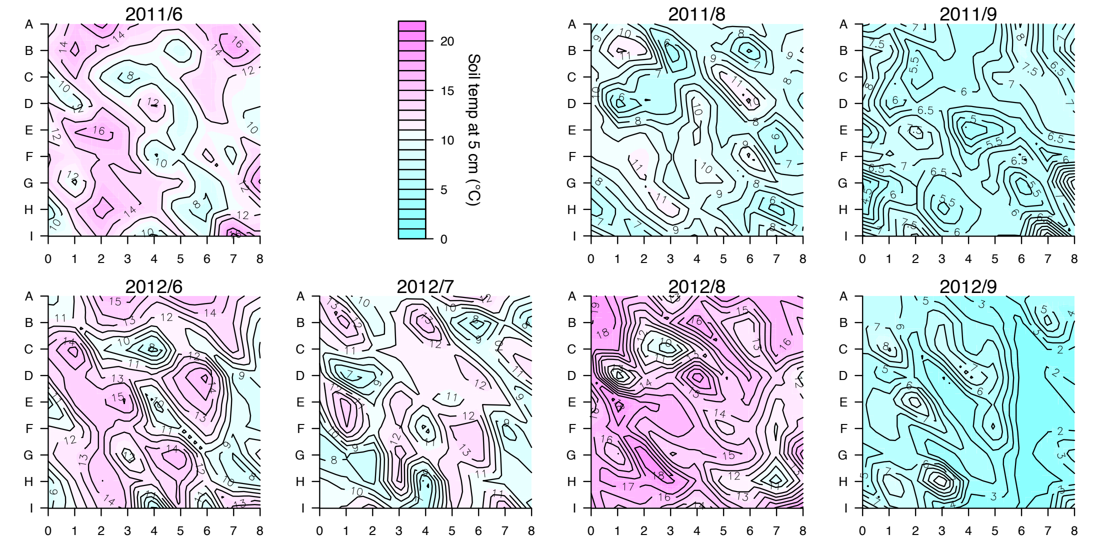

Fig. 3. Spatial distribution of soil temperature (°C) at 5 cm depth below the surface within the plot, Council, Seward Peninsula, Alaska during the growing seasons of 2011 and 2012. No data shown for July of 2011, as described in Fig. 2.

BGD
11, 5903–5939, 2014

Constraint of soil moisture on CO_2 efflux in tundra ecosystem

Y. Kim et al.

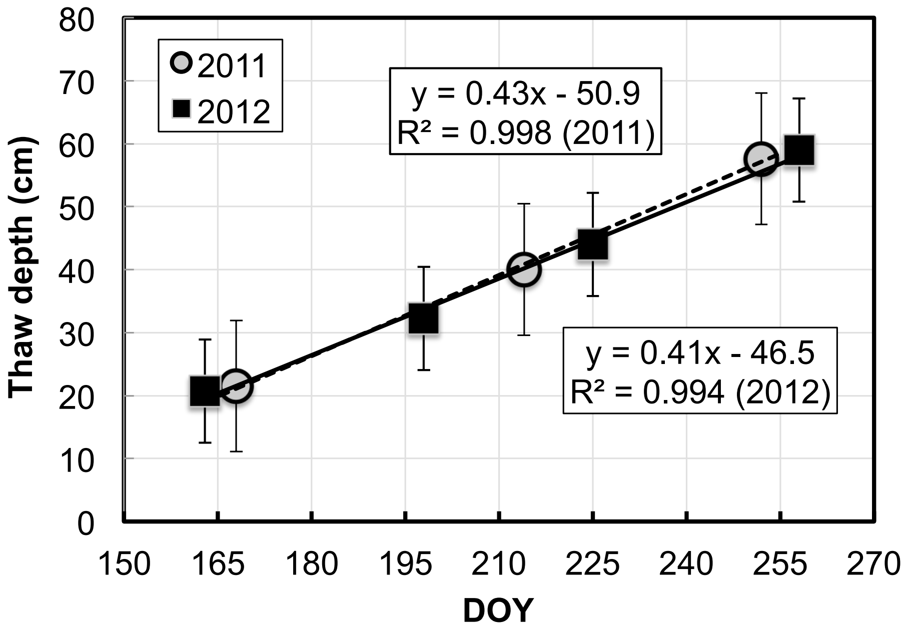

Fig. 4. Temporal variations in thaw depths in 2011 (circle) and 2012 (square) during the growing season, indicating that the thawing rates in active layers are 0.43 and 0.42 cm day^{-1}, respectively. Dashed and solid lines denote 2011 and 2012, respectively.

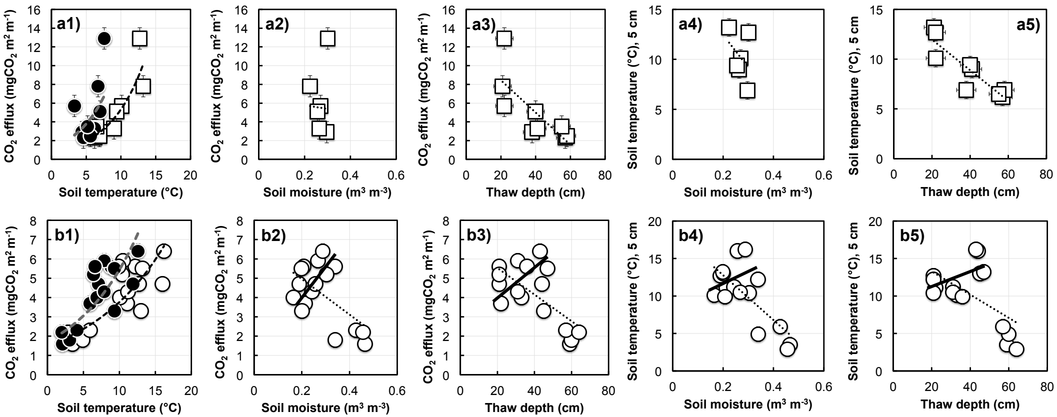

Fig. 5. Responses from monthly average CO_2 efflux to **(1)** average soil temperature at 5 and 10 cm (open and solid circles), **(2)** average soil moisture, and **(3)** thaw depth, and responses from average soil temperature at 5 cm to **(4)** average soil moisture and **(5)** average thaw depth during the growing seasons of **(a)** 2011 and **(b)** 2012. Dashed curves (**a1** and **b1**) and dotted lines indicate the relationship between both. Furthermore, solid lines in (**b2–5**) denote the relationship between both parameters, except for the data measured in September.

BGD
11, 5903–5939, 2014

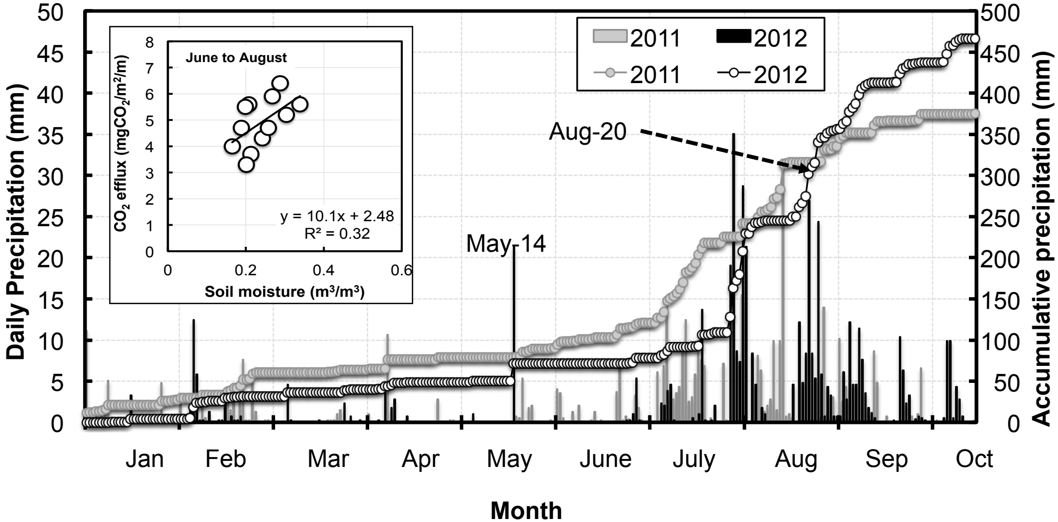

Fig. 6. Temporal variations of daily (bar) and accumulative precipitation (circle), January to October of 2011 and 2012. The response from CO_2 efflux to soil moisture from June to August of 2012 tends to increase with time; however, the response from June to September indicates a decreasing tendency since 20 August 2012, as shown in Fig. 5b2. This suggests the heavy rainfall event has a role in constraining soil CO_2 emission.

BGD
11, 5903–5939, 2014

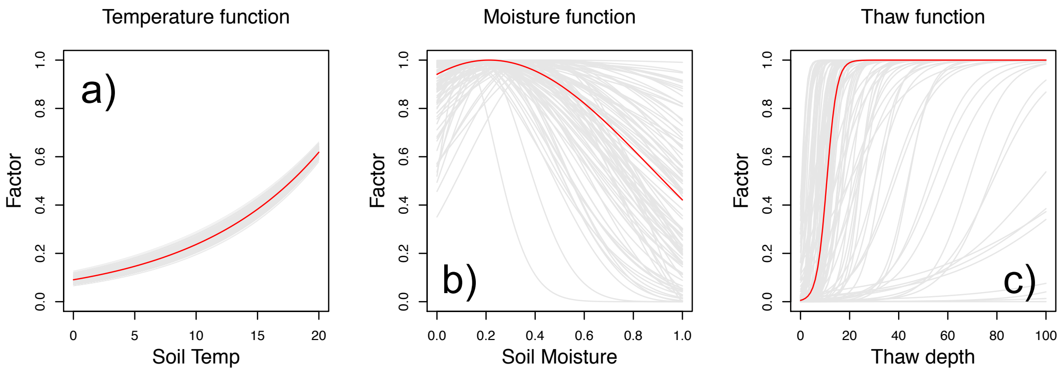

Fig. 7. Limiting functions for **(a)** soil temperature, **(b)** soil moisture, and **(c)** thaw depth of CO_2 efflux simulated by posteriors (n = 1000). Red solid lines are simulated from posterior median.

BGD

11, 5903–5939, 2014

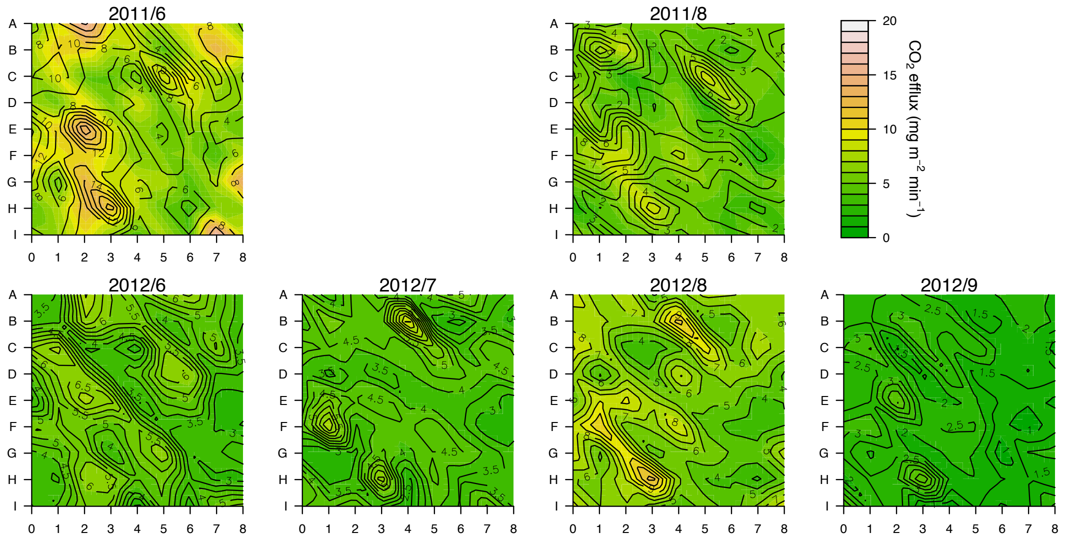

Fig. 8. Spatial distribution of simulated CO_2 efflux ($mg\,CO_2\,m^{-2}\,min^{-1}$) by posterior medians in HB model that is a function of soil temperature, soil moisture, and thaw depth within the plot, Council, Seward Peninsula, Alaska, during the growing seasons of 2011 (upper panel) and 2012 (lower).

BGD
11, 5903–5939, 2014

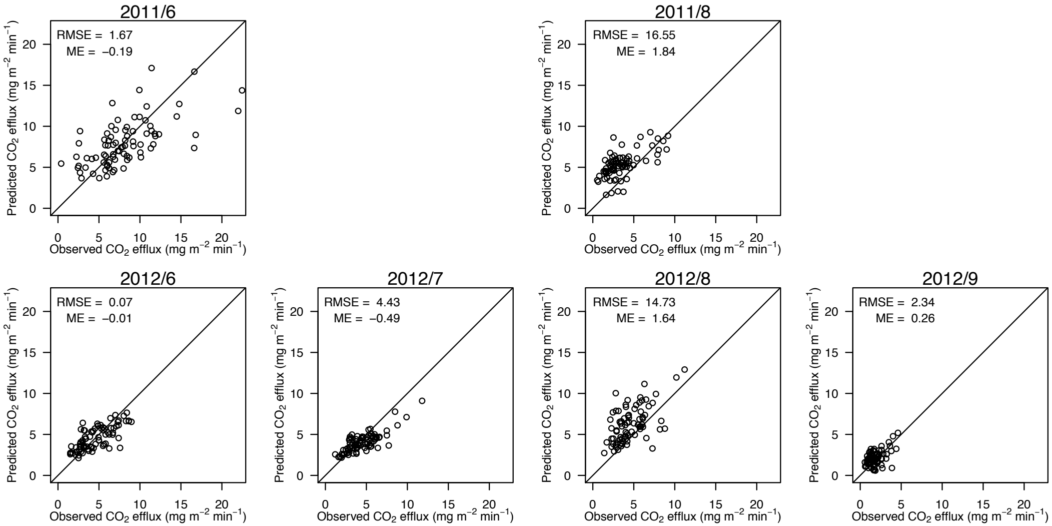

Fig. 9. Response of measured CO_2 efflux on simulated CO_2 efflux by posterior medians in HB model that is a function of soil temperature, soil moisture, and thaw depth within a 40 m × 40 m plot (5 m interval; 81 points), Council, Seward Peninsula, Alaska during the growing seasons of 2011 (upper panel) and 2012 (lower).

BGD
11, 5903–5939, 2014

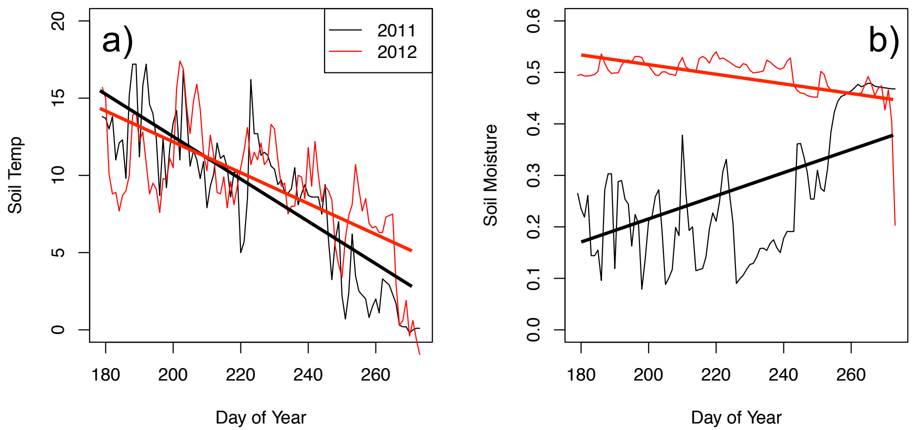

Fig. 10. Temporal variations of **(a)** soil temperature (°C) and **(b)** soil moisture ($m^3\,m^{-3}$), measured for tundra sites during the growing seasons of 2011 (black) and 2012 (red). When soil temperature was below zero, soil moisture drops rapidly at the end of September 2012, as shown in Fig. 1.

BGD
11, 5903–5939, 2014